

Numerical Modelling of Structural Glass Elements under Thermal Exposure

Chiara Bedon ^{1,*}, Daniel Honfi ² and Marcin Kozłowski ³

¹ University of Trieste, Italy; chiara.bedon@dia.units.it

² RISE Research Institutes of Sweden, Sweden; daniel.honfi@ri.se

³ Silesian University of Technology, Poland & Lund University, Sweden; marcin.kozlowski@polsl.pl

* Correspondence: chiara.bedon@dia.units.it; Tel.: +39-040-558-3837

Received: 24 April 2018; Accepted: 21 May 2018; Published: 21 May 2018

Abstract: Glass is largely used in engineering applications as a structural material, especially for laminated glass (LG) sections. However, the well-known temperature-dependent behaviour of visco-elastic interlayers for LG sections should be properly accounted for safety purposes, even in ambient conditions. The materials thermo-mechanical degradation with increase of temperature could further severely affect the load-bearing performance of such assemblies. Thermo-mechanical Finite Element (FE) numerical modelling, in this regard, can represent a robust tool and support for designers. Key input parameters and possible limits in FE models, however, should be properly taken into account and calibrated, especially for geometrically simplified models, to enable realistic and reliable estimations of real structural behavior. In this paper, FE simulations are proposed for monolithic (MG) and LG specimens under radiant heating, based on one-dimensional (1D) models. With the use of experimental results from the literature, parametric studies are discussed, indicating limits and issues at several modelling assumptions. Careful consideration is paid for various thermal material properties (conductivity, specific heat), boundary conditions (conductivity, emissivity) as well as geometrical features (thickness tolerances, etc.) and composition of LG sections (interlayer type, thickness). Comparative parametric results are hence discussed in the paper.

Keywords: structural glass; laminated glass; experiments; numerical modelling; one-dimensional (1D) models; thermal loading; material properties; thermo-mechanical performance

PACS: J0101

List of abbreviations

The following abbreviations are used in this manuscript (list in alphabetical order):

AN: Annealed (glass)

Exp: Exposed node

EVA: Ethylene Vinyl Acetate

FE: Finite Element

FT: Fully tempered (glass)

LG: Laminated glass

MG: Monolithic glass

MOE: Modulus of Elasticity

HS: Heat strengthened (glass)

PVB: Polyvinyl Butyral

SG: SentryGlas

TC: Thermocouple

TPS: Transient Plane Source

Unexp: Unexposed node

1. Introduction

Glass is increasingly used in buildings as a structural material for load bearing components like columns, beams and fins, plates for roofs and facades, as a major effect of aesthetic-related benefits [1-3]. However, its structural performance under loading and boundary conditions of technical interest for safe design purposes still requires investigations. Major issues are related to the material's intrinsic features, including the thermo-physical and mechanical properties and their sensitivity to ambient conditions. Special care should be spent in particular for extreme loads, due to impacts, natural hazards but also to severe temperature variations and fire (e.g. [4, 5]), see Figure 1.

The performance of glass under thermal heating attracted attention of several experimental research studies especially since the 50s, due to the consistent use of glass panels in windows and fenestrations. Most of those investigations, however, are related to the experimental assessment of thermal shock effects in soda lime silica glass, while only limited experimental studies are currently available for the thermo-physical and mechanical characterization of this constructional material, and even less are related to the experimental and/or numerical analysis of composite glass systems and assemblies under combined thermo-mechanical loads [5, 6].

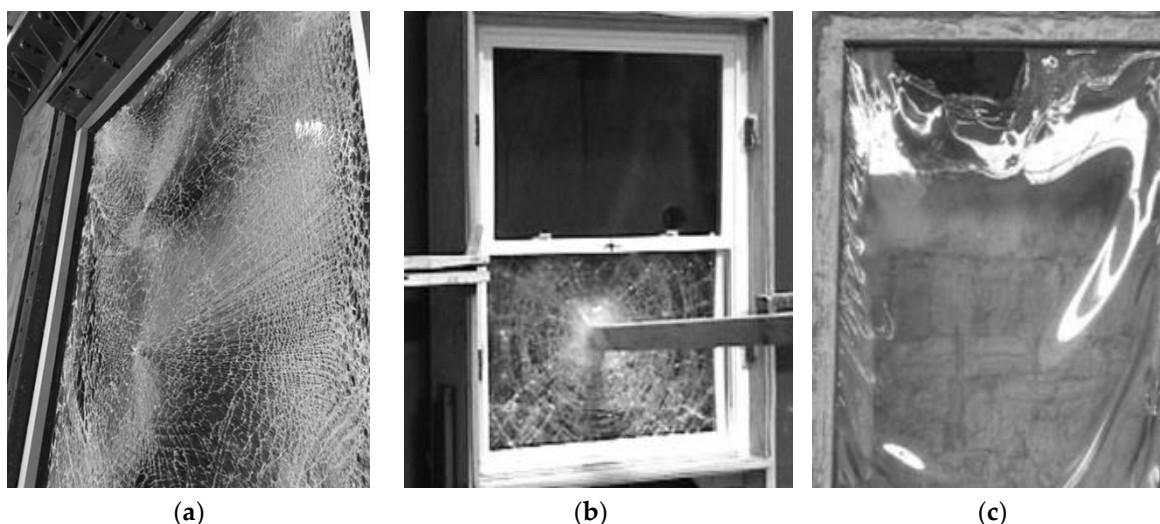


Figure 1. Examples of cracking and failure mechanisms in glass windows under (a) blast loading (photo adapted from [7]), (b) debris impact (adapted from [8]) and (c) fire (adapted from [5]).

This paper focuses on the performance evaluation of structural glass systems under thermal exposure, based on Finite Element numerical models [9] and past experimental tests [10, 11]. Simplified, one-dimensional (1D) models are considered at this stage of the study, as a part of ongoing extended investigations inclusive of bi-dimensional (2D) shell and tri-dimensional (3D) full solid models. As shown, careful consideration should be spent for the input material characterization to account for temperature effects. A certain sensitivity is however expected also from boundaries and size effects, that 1D models can only roughly describe. Numerical analyses are hence discussed for selected glass specimens under radiant heat flux, so to assess the accuracy and potential of 1D FE models.

In doing so, Section 2 briefly reports some key aspects for glass material under thermal loading, giving evidence of key influencing parameters that should be properly accounted for the FE assessment of the thermo-mechanical performance of glazing components and assemblies. Past reference experiments are then presented in Section 3, including a description of FE methods and assumptions. Based on the FE parametric results summarized in Section 4, some preliminary recommendations are then provided, as a part of an ongoing research study.

2. Material Properties and Temperature Effects

Glass is a material characterized by a MOE, in the range of 70GPa [12], and by a typical brittle elastic tensile behavior with limited effective strength. Although thermal or chemical pre-stressing processes can increase the reference characteristic tensile strength of AN glass (with 45MPa the nominal value [12]) by a factor of about two (for HS) or even three (in the case of FT glass), the occurrence of both local or global failure mechanisms due to the tensile peaks should be properly prevented.

Considerable attention should be given especially to LG cross-sections, representing the majority of structural glass applications but being typically characterized by the presence of two (or more) glass layers and one (or more) intermediate foils acting in the form of a flexible shear connection. Common interlayers are in fact composed of thermoplastic films like PVB, SG or EVA components, whose shear stiffness G_{int} is relatively low and depends on several conditions (e.g. time loading, temperature, humidity, etc.), see [1, 2]. Further issues in the load bearing performance of glazing systems are related to thermal loading, both inclusive of temperature gradients due to daily exposure and/or fire.

2.1. Specific Heat and Thermal Conductivity

Specific heat and thermal conductivity represent, from a numerical point of view, the first key input parameters for glass systems under thermal loads, especially when composite resisting sections consisting of LG panels are examined. However, literature references are rather limited for standard glass in use for civil engineering applications, and even more for the bonding interlayers. In this research study, input features are taken from past literature, see [10, 13, 14] and Figure 2.

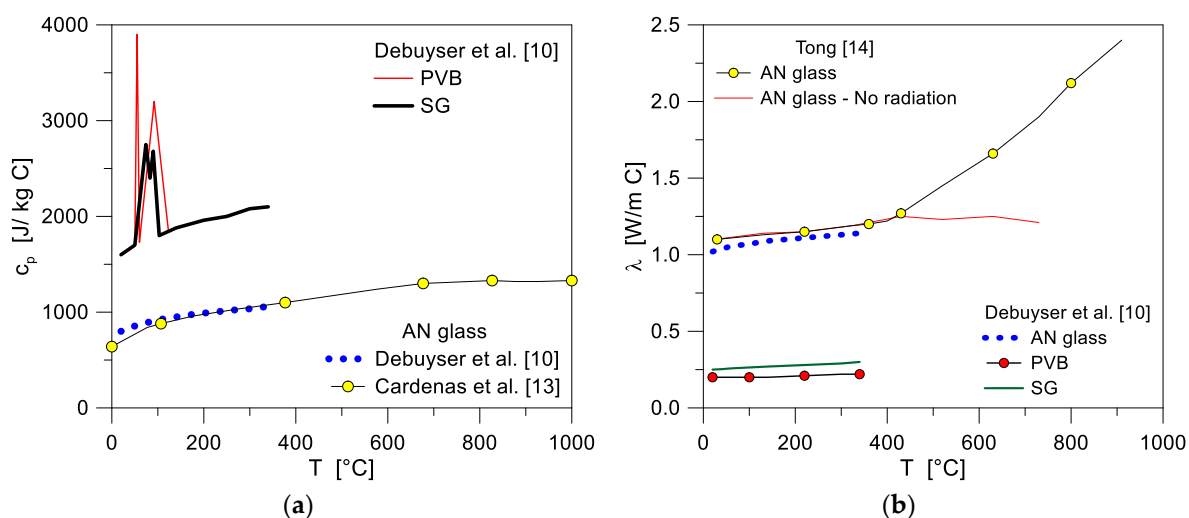


Figure 2. Thermal properties of glass as a function of temperature T : (a) specific heat c_p and (b) thermal conductivity λ .

2.2. Thermal Shock Performance

Generally speaking, thermal shock resistance in glass is conventionally estimated as a function of an allowable temperature gradient that the glass panels can withstand?. Such a temperature gradient - being affected by several geometrical and mechanical parameters, including the glass panels thickness, possible reinforcing (pre-stressing) and/or edge treatments, etc. - is conventionally accounted according to prEN thstr:2004 provisions [15] and can lie in the range from 22°C up to 200°C, see Table 1. As far these gradients are not exceeded, the glazing component should be able to withstand thermal shock.

Besides such a list of conventional values of interest for design purposes, see Table 1, a huge number of experimental studies related to the thermal performance and resistance of glass has been

focused on thermal breakage (see for example some recent studies in [16-20]), being representative of the major reason of glass cracking for windows and fenestrations. However, the topic still requires further studies, since even counterposed findings can be derived from past research projects [5].

Table 1. Allowable temperature gradients, according to prEN thstr:2004 [15].

Glass type	Limit values (°C)		
	As-cut or arrised	Smooth ground	Polished
Float or sheets ≤12mm thick	35	40	45
Float 15mm or 19mm thick	30	35	40
Float 25mm thick	26	30	35
Patterned		26	
Wired patterned or polished wired glass		22	
Heat strengthened		100	
Tempered		200	
Laminated	Smallest value of the component panes		

2.3. Mechanical Properties of Glass

A final key aspect for thermo-mechanical FE numerical analysis of glass systems is then represented by the degradation of the nominal mechanical features with temperature, namely the MOE and the tensile strength. The elastic properties of standard glass at elevated temperatures have been extensively assessed by several authors after the 50s, see for example [5] where a literature review is reported. Special care should be then spent especially for the numerical analysis of glazing systems interaction with different materials, including supports effects and possible local detailing (see for example [6]). In this research study, thermal phenomena are considered only.

3. Experimental and Numerical Studies

3.1. Reference Experimental Tests

Debuyser et al. [10, 11] investigated the behaviour of monolithic and triple layered LG specimens composed of AN glass bonded together by PVB or SG interlayers. Radiant panel tests and measurement of thermal properties of glass and interlayer materials were carried out. In the radiant panel tests, 285mm × 185mm monolithic and LG specimens were exposed to a heat source generating a relatively constant radiative heat flux (see Figure 3). During the tests, a central heat flux gauge measured the transmitted flux behind the glass; a side gauge, in plane with the glass surface, was exposed to the radiation directly; and the reflected heat flux was captured by a heat flux meter placed behind the radiant panel.

The typical experimental setup is presented in Figure 3(a), where the test frame, the central and the side heat flux gauges are seen covered with aluminium foil. Until a stable radiant heat flux had been achieved, an insulating board was placed in front of the radiant panel. After munting a glass panel, the board was removed and the glass sample was exposed to the radiant heat flux. At the end of each test, the glass panel was removed and the incident heat flux was measured at the position of the (previously removed) glass surface. Furthermore, the temperature evolution as a result of the heat

exposure was monitored during the test. Different thermocouple (TC) configurations were used to measure temperatures on both the exposed and the unexposed side of the glass panels. In case of some LG specimens TCs were also mounted between the glass plies embedded in the interlayers before lamination. To protect the TCs from direct radiation, on the exposed surface and in the interlayer, small pieces of aluminium tape were used for shielding.



Figure 3. Thermal experiments on glass specimens [10, 11]: (a) test setup (with LG sample) and (b) failed specimens.

In the measurement of thermal properties of glass and interlayers, thermal conductivity, diffusivity and volumetric heat capacity were experimentally determined using Transient Plane Source (TPS) measurements. The spectral transmittance and reflectance of a 6mm thick monolithic glass specimen was measured for a range of different wavelengths using spectrophotometers. Based on the results, the emissivity of glass is found to be moderately dependent on the considered spectrum. A spectrum-averaged value was determined by considering black-body distributions for a range of typical temperatures. For the interlayer materials (PVB and SG) the heat absorbed in the endothermic reactions were experimentally determined. For both interlayer materials, two endothermic peaks were observed. With the help of the area under the peaks and the slope defined by the start and end of the reaction the heat absorption could be determined.

In accordance with earlier research efforts, the relatively limited resistance and low thermal performance of AN glass specimens, due to the premature occurrence of thermal cracks as well as the poor thermal reaction of bonding interlayers, was observed. The typical crack patterns and bubbles formed in melting and evaporating interlayers can be observed in Figure 3(b).

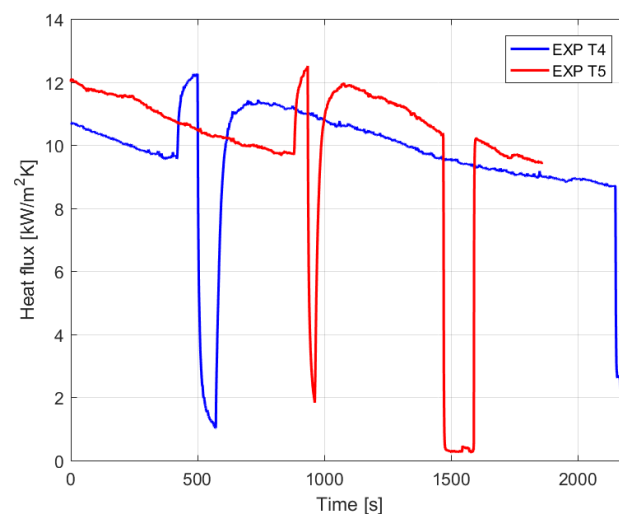


Figure 4. Measured heat flux (at the side) for specimens T4 and T5.

To develop and validate the numerical model (see Section 3.2), two test setups and results were selected (from the total set of 16 samples). The test denoted with T4 was a 15mm thick monolithic glass panel, whereas T5 was a laminated glass (6+10+6mm) specimen with a 0.76mm PVB interlayer. Besides the material parameters, the main input in such models is the heat flux to which the panels are exposed to. Since the incident heat flux was not directly measured, for the sake of simplicity, the heat flux measured by the heat flux meters at the side was used here.

The results of these measurements for specimens T4 and T5 are presented in Figure 4. From the trend lines it can be seen that the heat flux was not really stable and slightly decreasing with time. The jumps in the lines were due to a manual increase of the glass flow (to compensate for the steady decrease). The first sudden drops were caused by unintentional shutting off of the radiant panel. The final drops happened due to putting the insulation boards in place while removing the glass.

3.2. One-Dimensional (1D) Numerical Modelling

The main aim of the numerical study here summarized was to investigate the temperature evolution through the thickness of glass samples subjected to the assigned heat flux histories. Following the testing program reported in Section 3.1, a selection of both monolithic and LG panels was numerically analysed, by taking into account the experimentally heat flux data. In doing so, careful consideration was spent for some key influencing parameters, including sensitivity studies to investigate the effects due to variations in the surface and material thermal parameters.

The typical one-dimensional (1D) heat transfer model, similar to those presented in [10, 11] was created using the commercial computer software ABAQUS [9], see Figure 5. It consisted in 2-node, 1-dimensional diffusive heat transfer elements (DC1D2 type from ABAQUS library).

Thermal properties of glass and interlayers, such as conductivity and specific heat were taken from literature projects recalled in Section 2.1. A reference emissivity coefficient equal to 0.97 was assumed for the glass surface. Density of glass equal to 25 kN/m² was finally accounted in the study [12]. According to Figure 5, the thermal exposure was simulated by applying a concentrated heat flux to the exposed node, including heat flux vs. time amplitudes from the experiments, see Section 3.1. An initial ambient temperature of 20°C was applied to the model. In all the FE thermal simulations, moreover, the following physical constants were considered:

- Stefan-Boltzmann constant ($5.67 \times 10^{-8} \text{ W/m}^2\text{K}^{-4}$),
- absolute zero temperature (-273°C).

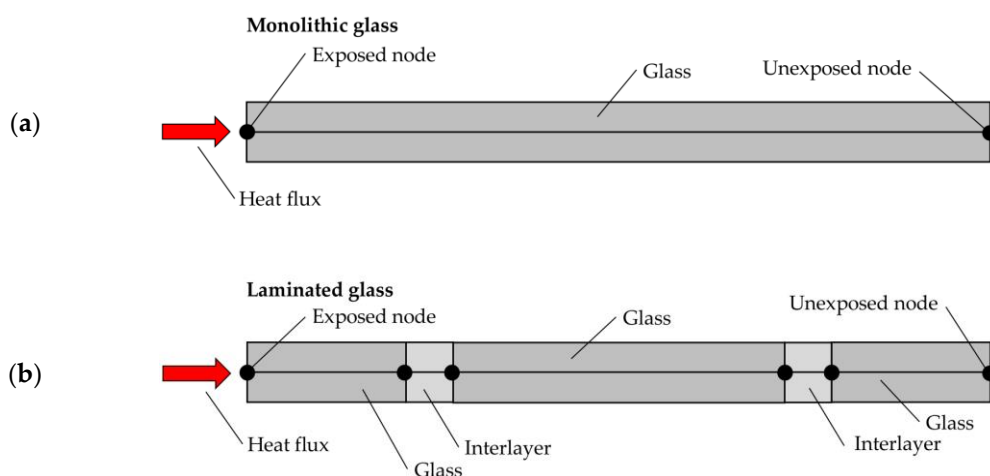


Figure 5. Schematic representation of 1D heat transfer models: (a) monolithic and (b) laminated specimens.

A Fortran script user-subroutine was finally utilized to define the boundary conditions between external nodes and the surrounding environment. This included a convective heat transfer coefficient (h) dependent on the varying temperature of exposed and unexposed nodes [21].

The h coefficient is dependent on the fluid properties (thermal conductivity, density and viscosity), flow parameters (velocity and nature of the flow) and the geometry of the sample (dimensions and angle to the flow). It can be expressed in terms of Grashof and Prandtl dimensionless groups that allow the physical properties of the fluid, the flow velocity and nature of convection to be taken into account. The Grashof dimensionless group G_r is conventionally expressed as:

$$G_r = \frac{g l^3 \beta (T_1 - T_0)}{\nu^2} \quad (1)$$

where g is the gravitational acceleration constant (9.81 m/s^2), l is the flame height (0.185 m), β is the coefficient of air expansion ($3.41 \times 10^{-3} \text{ 1/K}$), T_0 is the initial (ambient) temperature, T_1 is the current temperature, ν is the kinematic viscosity ($1.51 \times 10^{-5} \text{ m}^2/\text{s}$). Air properties at 20°C were taken from [22]. The Prandtl dimensionless group P_r is then expressed as:

$$P_r = \frac{\nu}{\alpha} \quad (2)$$

where α is the air thermal diffusivity ($2.11 \times 10^{-5} \text{ m}^2/\text{s}$).

The h coefficient is hence defined by the product of Prandtl and Grashof numbers, and for a vertical plate with natural, laminar convection is given by:

$$h = \frac{k \cdot 0.59 (G_r \cdot P_r)^{1/4}}{l} \quad (3)$$

where k is the thermal conductivity of air (0.026 W/mK). Typically, h takes values in the range of 5–50 $\text{W/m}^2\text{K}$ for natural convection [23].

Based on the 1D models shown in Figure 5, an overview of parametric configurations discussed in this work is summarized in Table 2. Regarding monolithic glass, firstly, the effects of varying emissivity and film surface coefficient were investigated. Secondly, parametric studies were focused on the variation of the nominal glass thickness, including manufacturing tolerances ($\pm 0.5\text{mm}$ for 15mm glass thickness, see [24]). In terms of LG samples, different thicknesses of PVB interlayer were also taken into account.

Table 2. Thermal and geometrical properties for the 1D parametric models (ABAQUS). US= user sub-routine.

	Model	Glass thickness		Emissivity	Film coefficient	Interlayer thickness / type
		/build-up	[mm]			
Emissivity & Film coefficient	MG-E0.97	15	0.97	0.97	US	-
	MG-E0.84	15	0.84	0.84	US	-
	MG-FC-8.02	15	0.84	8.02	US	-
Glass thickness	MG-THK-14.5	14.5	0.97	0.97	US	-
	MG-THK-15.5	15.5	0.97	0.97	US	-
Interlayer	LG-PVB-0.76	6+10+6	0.97	0.97	US	0.76 mm / PVB
	LG-PVB-1.52	6+10+6	0.97	0.97	US	1.52 mm / PVB

4. Discussion of FE Numerical Results and Assessment to Experiments

Figure 6 presents a comparison of numerical and experimental results for the MG specimen T4. The figure illustrates the influence of variations of (i) glass emissivity, (ii) constant and temperature dependent film surface coefficient and (iii) glass thickness (by taking into account dimensional tolerances) on the T4 thermal response.

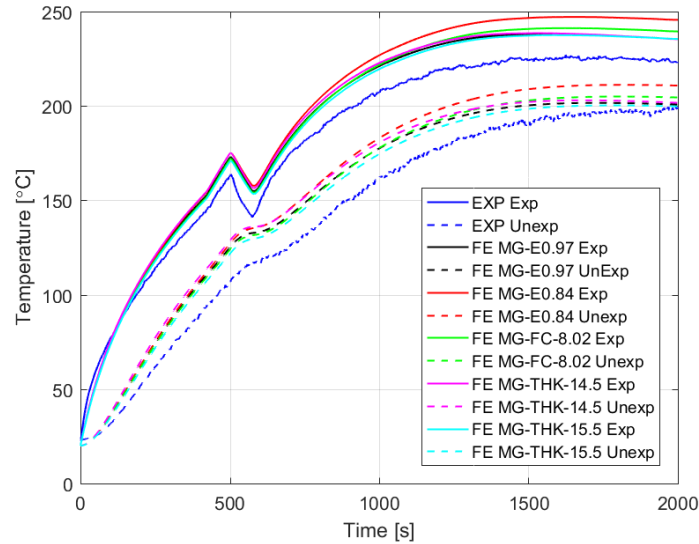


Figure 6. Temperature history comparison between FE parametric analyses and experimental results, for the MG specimen T4. Continuous lines represent the temperature history at the node exposed to heat flux (Exp), while dashed lines are for the unexposed node (UnExp).

In general, the FE numerical results were observed to slightly overestimate the experimental data, see Figure 6. Much better correlation was found especially at the beginning of the temperature history, for the model node exposed to the heat flux, rather than at the later stage of the analysis (where the FE temperature values present no more than 12% scatter). In the case of the unexposed node, for the whole simulation time, the FE results were indeed found to overestimate the experimentally measured temperatures, by approx. 10%. Minor effects due to variation of glass emissivity and/or film surface coefficient were found, and such an outcome applies especially to the early stage of the analyses (up to approx. 800s of thermal loading).

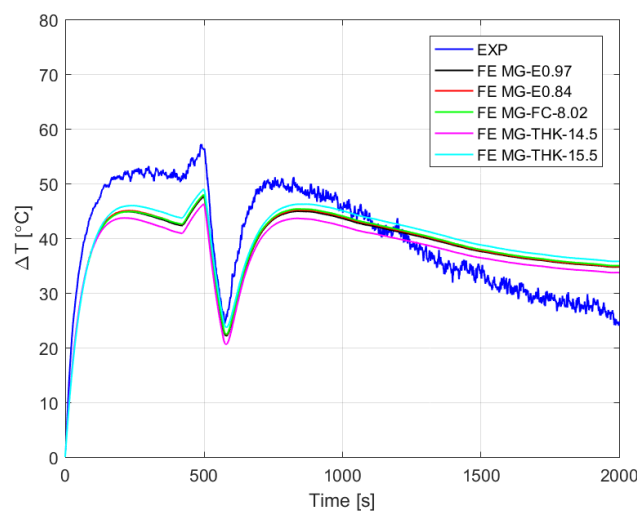


Figure 7. Temperature gradient DT history comparison between FE parametric analyses and experimental results, for the MG specimen T4.

Figure 7 presents the temperature gradient ΔT for the same T4 sample, as derived from the thermal responses measured at external nodes of glass (i.e. exposed and unexposed to the assigned heat flux). As shown, the numerical results were observed to underestimate the experiments until approx. 1200s of exposure, while subsequently the FE predictions overestimate the experiments. Since the temperature gradient is strictly related to potential failure of glass due to thermal shock phenomena (see Table 1), careful attention should be spent on this aspect.

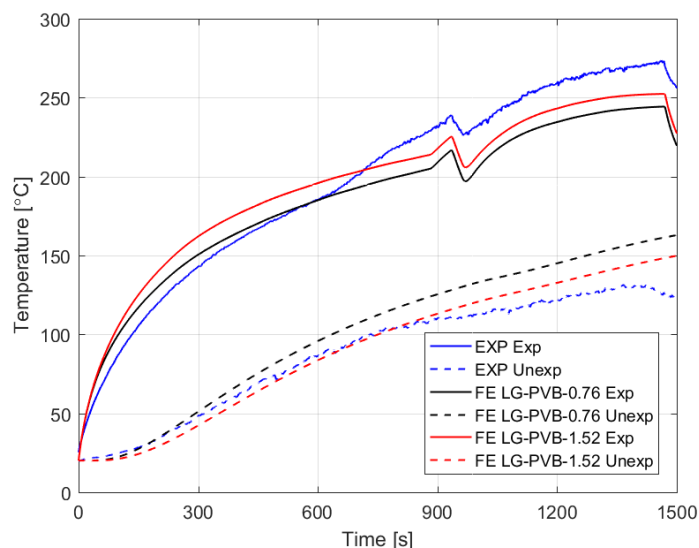


Figure 8. Temperature history comparison between FE parametric analyses and experimental results, for the LG specimen T5. Continuous lines represent the temperature history at the node exposed to heat flux (Exp), while dashed lines are for the unexposed node (UnExp).

Figure 8, finally, presents a comparison of numerical and experimental results for the LG specimen T5. The analyses were focused on the influence of varying thickness of PVB interlayer. Similar to the specimen T4, much better agreement with the experiments was observed for the early stage of the FE analyses. This includes the temperature evolution at both – the exposed and unexposed – model nodes. As shown, small variations in the PVB thickness typically resulted in increased temperature at the exposed node and reduced temperature at the unexposed node, compared to the reference geometrical configuration.

5. Conclusions

The paper presents the first steps of the development of a reliable thermo-mechanical model of structural glass at elevated temperatures. Although the current model includes a number of simplifications and focuses on the heat transfer only, several interesting conclusions can be drawn from the process of the development and from the numerical results obtained.

One difficulty is that limited information exists on the temperature dependence of various material properties of glass, and if does, it is typically for a limited range of temperatures. Taking values directly from the literature references is often difficult, since the limitations of different values and empirical formulas are often not clearly stated. Therefore, performing tests in parallel with the development of numerical models can be extremely beneficial, since first hand information about the experiments exist and can be directly implemented.

Performing tests at elevated temperature is not an easy task and includes several uncertainties. For example, changes in the environment, i.e. opening a door in the lab can have a noticeable influence on the results. In case of testing glass panels, even the measurement of the temperatures involves various challenges. The TCs, their shielding from direct heat flux and wires all obstruct the transparency of glass and can create local disturbances in the temperature distribution. Therefore, it

is not obvious which of the measured temperature is most relevant for comparison with the numerical model. The same applies for the heat flux measurement, since the incident heat flux cannot be directly measured. Due to these difficulties, the authors defined an approach in which from a geometrically simplified 1D heat transfer model, more detailed 2D and 3D numerical models inclusive of size and boundary effects are gradually extended. A further step is then to expand the model to account for the thermo-mechanical behaviour of glass.

Acknowledgments: Part of the research study discussed in this research paper has been financially supported by the EU-COST Action TU1403 “Adaptive facades network” (2014-2018, www.tu1403.eu), in the form of short-term scientific mission grants for the involved authors (Dr. Kozłowski visiting University of Trieste, Italy, and Dr. Bedon visiting RISE, Sweden). For this reason, COST is gratefully acknowledged, since facilitating the scientific networking between the Early Career researchers.

Author Contributions: The current research paper results from an ongoing collaboration between the authors. Dr. Honfi was actively involved in the past experimental study, while Dr. Bedon and Dr. Kozłowski handled the FE numerical simulations. Finally, all the authors actively supported the interpretation of FE results and the critical discussion of comparison with past experimental tests.

Conflicts of Interest: The authors declare no conflict of interest.

References

1. Haldimann, M.; Luible, A.; Overend, M. *Structural use of glass*. IABSE, ISBN 978-3-85748-119-2, 2008
2. Feldmann, M.; Kasper, R.; Abeln, B.; Cruz, P.; Belis, J.; et al. *Guidance for European Structural design of glass components – support to the implementation, harmonization and further development of the Eurocodes*. Report EUR 26439, Joint Research Centre–Institute for the Protection and Security of the Citizen, doi: 10.2788/5523, Pinto Dimova, Denton Feldmann (Eds.), 2014
3. Buildings Department. *Code of Practice for Structural Use of Glass 2018*. Available online: www.bd.gov.hk/english/documents/coee/SUG2018e.pdf (accessed April 24th, 2018)
4. Bedon, C.; Zhang, X.; Santos, F.; Honfi, D.; Kozłowski, M.; Arrigoni, M.; Figuli, M.; Lange, D. Performance of structural glass facades under extreme loads – Design methods, existing research, current issues and trends. *Construction and Building Materials*, 2018, 163: 921-937
5. Bedon, C. Structural glass systems under fire: overview of design issues, experimental research, and developments. *Advances in Civil Engineering*, Volume 2017, Article ID 2120570, 18 pages. Available online (accessed April 24th, 2018): <https://doi.org/10.1155/2017/2120570>
6. Bedon, C.; Louter, C. Thermo-mechanical numerical modelling of structural glass under fire - Preliminary considerations and comparisons. *Proceedings of Challenging Glass 6 - Conference on Architectural and Structural Applications of Glass*, Delft University of Technology, The Netherlands (USB drive), 2018
7. *Campbell Window Film - How to Survive a Bomb Blast*. Available online (accessed April 24th, 2018): https://www.youtube.com/watch?v=qKNVJb6Ls_E
8. *Ester Shower Glass & Window - Hurricane Impact Windows*. Available online (accessed April 24th, 2018): <http://esteroglasscompany.com/windows/hurricane-impact-windows/>
9. Simulia. ABAQUS v. 6.14 computer software and online documentation, Dassault Systems, Providence, RI, USA
10. Debuyser, M.; Sjöström, J.; Lange, D.; Honfi, D.; Sonck, D.; Belis, J.. Behaviour of monolithic and laminated glass exposed to radiant heating. *Construction and Building Materials*, 2017, 130: 212–229
11. Debuyser, M. *Exploratory investigation of the behaviour of structural glass in fire*. Master Dissertation, Ghent University, Belgium, 2015
12. EN 572-2: 2004. *Glass in buildings – basic soda lime silicate glass products*, CEN, Brussels, Belgium
13. Cardenas, B.; Leon, N.; Pye, J.; Garcia, H.D. Design and modeling of high temperature solar thermal energy storage unit based on molten soda lime silica glass. *Solar Energy*, 2016, 126: 32–43
14. Tong, T.W. *Thermal Conductivity 22*, Technomic Publishing Company, Ltd., Lancaster, PA, USA, 1994, ISBN 1-56676-172-7
15. prEN thstr:2004. *Glass in Buildings - thermal stress capitulation method*, CEN, Brussels, Belgium
16. Mognato, E.; Barbieri, A. The breakage of glass - Thermal shock and nickel sulfide inclusions. *Proceedings COST Action TU0905 Mid-term Conference on Structural Glass*, ISBN 978-1-138-00044-5, 2013

17. Malou, Z.; Hamidouche, H.; Bouaouadja, N.; Chevalier, J.; Fantozzi, G. Thermal shock resistance of a soda lime glass. *Ceramics–Silikáty*, 2013, 57(1): 39–44
18. Vandebroek, M. Thermal Fracture of Glass. Ph.D. Dissertation, Ghent University. Available online (accessed April 24th, 2018): <https://biblio.ugent.be/publication/5757540/file/5757541>, ISBN 978-90-8578-738-9, 2015
19. Karlsson, S. Spontaneous fracture in thermally strengthened glass - A review and outlook. *Ceramics-Silikáty*, 2017, 61(3): 188-201, doi: 10.13168/cs.2017.0016
20. Wang, Q.; Chen, H.; Wang, Y.; Sun, J. Thermal shock effect on the glass thermal stress response and crack propagation. *Procedia Engineering*, 2013, 62: 717-724
21. Drysdale, D. An introduction to fire dynamics Dougal Drysdale, Oxford : Wiley-Blackwell, 2011
22. Microelectronics Heat Transfer Laboratory - Fluid Properties Calculator. Available online (accessed April 24th, 2018): <http://www.mhtl.uwaterloo.ca/old/onlinetools/airprop/airprop.html>
23. Tolerances handbook 06/2014, Saint-Gobain, 2014 ECKELT GLAS GmbH. Available online (accessed April 24th, 2018): http://www.eckelt.at/en/downloads/produkte/tolerances_handbook.pdf
24. Welty, J.R.; Wicks, C.E.; Wilson, R.E.; Rorrer, G. Fundamentals of Momentum, Heat and Mass Transfer, 5th edn. John Wiley & Sons, Inc., New York, 2008

© 2018 by the authors; licensee MDPI, Basel, Switzerland. This article is an open access article distributed under the terms and conditions of the Creative Commons Attribution (CC BY) license (<http://creativecommons.org/licenses/by/4.0/>).

